

FitMultiCell: Simulating and parameterizing computational models of multi-scale and multi-cellular processes

Emad Alamoudi¹, Yannik Schälte^{1,2,3}, Robert Müller⁴, Jörn Starruß⁴,
Nils Bundgaard⁵, Frederik Graw^{5,6,7}, Lutz Brusch⁴, Jan Hasenauer^{1,2,3,*}

February 21, 2023

¹ Life and Medical Sciences Institute, University of Bonn, 53113 Bonn, Germany, ² Helmholtz Zentrum München - German Research Center for Environmental Health, Institute of Computational Biology, 85764 Neuherberg, Germany, ³ Technische Universität München, Center for Mathematics, Chair of Mathematical Modeling of Biological Systems, 85748 Garching, Germany, ⁴ Center of Information Services and High Performance Computing (ZIH), Technische Universität Dresden, 01062 Dresden, Germany, ⁵ BioQuant - Center for Quantitative Biology, Heidelberg University, 69120 Heidelberg, Germany. ⁶ Interdisciplinary Center for Scientific Computing, Heidelberg University, 69120 Heidelberg, Germany, ⁷ Friedrich-Alexander-University Erlangen-Nürnberg, Department of Medicine 5, 91054 Erlangen, Germany

*To whom correspondence should be addressed.

Abstract

Motivation: Biological tissues are dynamic and highly organized. Multi-scale models are helpful tools to analyze and understand the processes determining tissue dynamics. These models usually depend on parameters that need to be inferred from experimental data to achieve a quantitative understanding, to predict the response to perturbations, and to evaluate competing hypotheses. However, even advanced inference approaches such as Approximate Bayesian Computation (ABC) are difficult to apply due to the computational complexity of the simulation of multi-scale models. Thus, there is a need for a scalable pipeline for modeling, simulating, and parameterizing multi-scale models of multi-cellular processes.

Results: Here, we present FitMultiCell, a computationally efficient and user-friendly open-source pipeline that can handle the full workflow of modeling, simulating, and parameterizing for multi-scale models of multi-cellular processes. The pipeline is modular

29 and integrates the modeling and simulation tool Morpheus and the statistical infer-
30 ence tool pyABC. The easy integration of high-performance infrastructure allows to
31 scale to computationally expensive problems. The introduction of a novel standard
32 for the formulation of parameter inference problems for multi-scale models additionally
33 ensures reproducibility and reusability. By applying the pipeline to multiple biologi-
34 cal problems, we demonstrate its broad applicability, which will benefit in particular
35 image-based systems biology.

36 **Availability:** FitMultiCell is available open-source at [https://gitlab.com/fitmulticell/](https://gitlab.com/fitmulticell/fit)
37 `fit`.

38 **Contact:** jan.hasenauer@uni-bonn.de

39
40 **Supplementary information:** Supplementary data are available at [https://doi.org/](https://doi.org/10.5281/zenodo.7646287)
41 `10.5281/zenodo.7646287` online.

42 1 Introduction

43 Biological tissues are complex entities composed of cells and extracellular components. Tis-
44 sues occur in different developmental stages and compositions, are highly dynamic and often
45 heavily structured. Specific tissue properties are relevant for a broad range of processes,
46 including tissue homeostasis, viral infection, and tumor development and treatment. For
47 the experimental analysis of biological tissues, imaging techniques are widely used. Com-
48 mon approaches include light and fluorescence microscopy, but more recently also imaging
49 mass cytometry, spatial transcriptomics and related methods are employed (see Lewis et al.
50 [2021] for a review). These experimental techniques provide a variety of quantitative infor-
51 mation about biological tissues. Yet, mechanisms underlying specific pattern formation or
52 tissue dynamics often remain elusive. To address these aspects, computational modeling has
53 established itself as a key element to obtain a comprehensive understanding of causal rela-
54 tionships in multi-cellular spatio-temporal systems. Computational models of multi-cellular
55 processes usually capture multiple spatial and temporal scales and describe the emergence
56 of the system's behavior based on individual building blocks, e.g. individual cells and their
57 interactions. There are several modeling approaches, including discrete, continuous and hy-
58 brid model formalisms [Anderson and Quaranta, 2008, Meyer et al., 2020, Waclaw et al.,
59 2015]. Cells and their interactions can, for instance, be described using (energy-based) Cel-
60 lular Potts Models (CPM) or (force-based) vertex models. Several software packages have
61 been developed, including MCell [Kerr et al., 2008], FLAME [Richmond et al., 2010], Com-
62 puCell3D [Swat et al., 2012], Chaste [Mirams et al., 2013], Morpheus [Starruß et al., 2014],
63 and PhysiCell [Ghaffarizadeh et al., 2018] to simplify and standardize the demanding task of
64 model formulation and implementation. Yet, while computational modeling has substantially
65 improved the understanding of multi-cellular systems, it remains a challenging task [Fletcher

66 and Osborne, 2022].

67 For multi-scale models of multi-cellular processes a key challenge is parameter estimation,
68 the process in which values for the unknown model parameters are determined by fitting the
69 model simulations to experimentally observed data. Parameter estimation is necessary to ob-
70 tain quantitative models of processes, to analyse processes, to compare competing hypotheses
71 about processes, and to predict the dynamics of processes (e.g., in response to perturbations)
72 [Durso-Cain et al., 2021, Imle et al., 2019, Jagiella et al., 2017, MacLean et al., 2014, Toni
73 et al., 2011]. Systematic, rigorous and uncertainty-aware parameter estimation is only just
74 becoming accessible for multi-scale models with advanced methods and growing computa-
75 tional resources. Reasons for this are that (i) the simulation of multi-scale models accounts
76 for different biophysical processes (e.g., intra- and extracellular signalling as well as physi-
77 cal interaction), which requires computationally efficient simulation algorithms (e.g., hybrid
78 discrete-continuum approaches), and that (ii) the stochasticity of most models (e.g. due to
79 randomness arising from small cell numbers) necessitates repeated simulations.

80 To cope with the challenges of parameter estimation for advanced computational models, Ap-
81 proximate Bayesian Computation (ABC) methods have been developed and applied [Beau-
82 mont et al., 2002, Pritchard et al., 1999, Sisson et al., 2018]. These methods generate samples
83 from an approximation of the Bayesian parameter posterior distribution, without evaluating a
84 likelihood function which can quickly become inaccessible for complex stochastic models. To
85 enable the application of ABC methods to multi-scale models, they have been parallelized on
86 high-performance computing (HPC) infrastructure [Babtie and Stumpf, 2017, Jagiella et al.,
87 2017, Johnston et al., 2014, Sottoriva et al., 2015]. Generic implementations are provided
88 by, in particular, pyABC [Klinger et al., 2018], ABCpy [Dutta et al., 2017], and ELFI [Kan-
89 gasrääsiö et al., 2016]. Yet, while simulation and inference tools are available, the parameter
90 estimation for multi-scale models of multi-cellular processes still requires a high level of tech-
91 nical expertise. The available tools are not interfaced and code from published application
92 examples is often difficult to reuse and extend. Thus, there is a need for a platform that
93 facilitates and streamlines the entire workflow, from the construction of multi-scale models
94 of various types based on biological principles, to systematic uncertainty-aware data-driven
95 parameter estimation [Hasenauer et al., 2015].

96 In this work, we introduce the FitMultiCell pipeline, an open-source, user-friendly, and scal-
97 able end-to-end platform that integrates modeling, simulation, and parameter estimation,
98 to simplify the analysis of multi-scale and multi-cellular systems. FitMultiCell integrates
99 the state-of-the-art tools Morpheus [Starruß et al., 2014] for model building and simulation,
100 and pyABC [Schälte et al., 2022] for parameter estimation. It builds on an extension of
101 the PEx standard [Schmiester et al., 2021] for the specification of parameter estimation
102 problems which we additionally introduce in this manuscript. We demonstrate and evaluate
103 the FitMultiCell pipeline using models for tumor growth and liver regeneration.

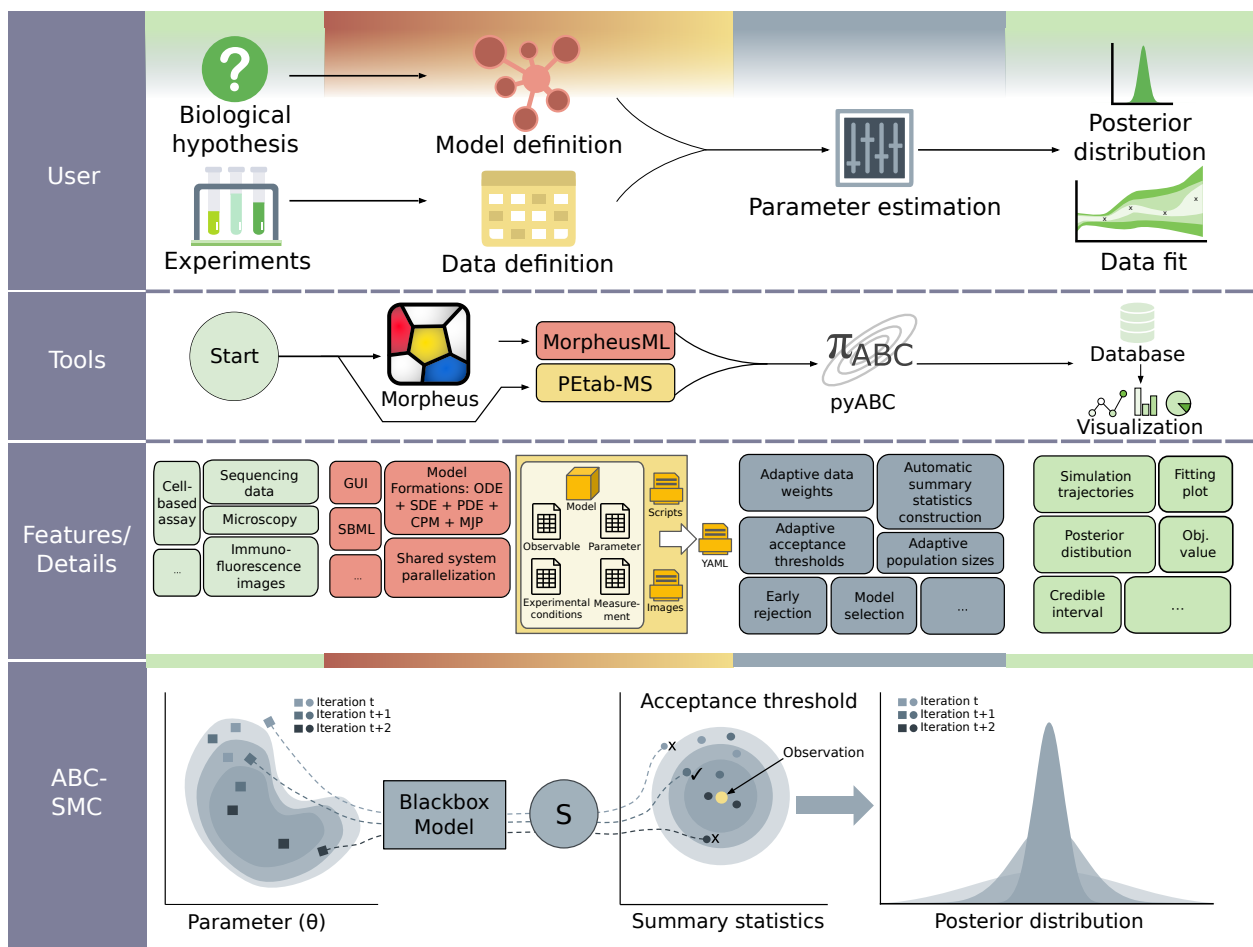


Figure 1: Overview of the FitMultiCell pipeline. First row: User perspective on the biological system, experiment, model formulation, and parameter estimation problem. Second row: Tool and format overview. Third row: Features and details for all components of the workflow. Fourth row: Visualization of the ABC-SMC parameter estimation algorithm.

2 Methods

2.1 Problem description

We consider the problem of developing quantitative computational models of multi-cellular processes. These models might account for a broad range of biochemical and biophysical processes, including

- cellular signal transduction, metabolism and gene regulation,
- cell movement, proliferation and death, and
- cell-cell communication (e.g., via direct cell-cell-contact areas or the secretion/uptake

112 of biochemical substances).

The spectrum of modeling frameworks for such integrated processes is broad and the models are often stochastic, like the behaviours and decisions by individual biological cells are inherently stochastic. Mathematically, we can write any such model as

$$y = \mathcal{M}(\theta, \xi),$$

113 where y denotes the vector of observed properties and θ denotes the vector of unknown
114 properties of biochemical, biophysical or observation processes (e.g. reaction rates). Process
115 noise – arising, for instance, from low molecular numbers – as well as measurement noise
116 is described via the vector of random variables ξ . Marginalizing the model simulation over
117 the random variables ξ yields the likelihood $\pi(y|\theta)$, which is the conditional probability of
118 observing y given θ .

Quantitative mathematical modeling requires the inference of the unknown parameters θ from data. In this study, we consider Bayesian inference and aim to approximate the Bayesian posterior distribution

$$\pi(\theta|y_{\text{obs}}) \propto \pi(y_{\text{obs}}|\theta) \cdot \pi(\theta)$$

119 of the unknown model parameters for experimentally observed data y_{obs} and prior knowledge
120 $\pi(\theta)$. The posterior distribution encodes all available information about the model parameter
121 and, hence, allows for the assessment of parameter and prediction uncertainties as well as
122 for the design of validation experiments. Experimental data used for the parameterization
123 of the considered models are often obtained using imaging techniques. These can provide
124 information about e.g. spatial profile, temporal changes and changes between conditions.
125 Overall, the spectrum of experimental setups is broad.

126 **2.2 FitMultiCell pipeline**

127 To facilitate quantitative computational modeling of multi-cellular processes, we developed
128 the FitMultiCell pipeline (Figure 1). This pipeline supports its users in

129 (1) formulating the modeling problem, i.e.

130 (a) defining computational models and

131 (b) defining data obtained from experiments,

132 (2) estimating unknown model parameters, and

133 (3) evaluating parameter and model predictions (including planning validation experi-
134 ments).

135 The FitMultiCell pipeline streamlines the parameter estimation process by providing a tight
136 integration of tools for model specification and simulation, and parameter estimation and re-
137 porting. This is achieved using a Python interface with a broad spectrum of functionalities.
138 The current version supports (1) multi-scale modeling and simulation using Morpheus [Star-
139 ruß et al., 2014], and (2) parameter estimation and uncertainty quantification using pyABC
140 [Klinger et al., 2018]. These state-of-the-art tools cover a broad spectrum of modeling ap-
141 plications; yet, other tools for modeling, simulation and parameter estimation can be easily
142 interfaced.

143 The FitMultiCell pipeline enables parameter estimation for application problems with mul-
144 tiple experimental conditions, data sets and data types. Furthermore, it offers a broad range
145 of built-in visualization and analysis tools. To facilitate reproducibility and reusability, the
146 FitMultiCell pipeline supports the MorpheusML and the P_Etab-MS standards.

147 In the following, we describe the key components of the FitMultiCell pipeline and their
148 features.

149 **2.2.1 Standardization**

150 The FitMultiCell pipeline uses standardized data formats to ensure interoperability, repro-
151 ducibility and reusability – important aspects of the FAIR principles [Wilkinson et al., 2016].
152 The multi-cellular models are encoded using MorpheusML, an established XML-based stan-
153 dard at <https://doi.org/10.25504/FAIRsharing.78b6a6>. The parameter estimation prob-
154 lems are encoded using the P_Etab-MS format, a newly developed tsv-file-based standard.

155 We developed P_Etab-MS as an extension of the Parameter Estimation tabular format (P_Etab)
156 [Schmiester et al., 2021], which was developed in the field of ordinary differential equation
157 (ODE) based modeling and is already supported by various simulators and parameter esti-
158 mation toolboxes. P_Etab-MS conserves most core components of P_Etab, including the tables
159 defining model parameters and experimental conditions. Yet, P_Etab-MS allows for model ex-
160 pression using MorpheusML, flexible data tables (including references to image files), as well
161 as functions for computing summary statistics. These aspects are essential for multi-cellular
162 processes and were not captured by P_Etab. The specification of P_Etab-MS and a tool for the
163 validation of files can be found at [https://gitlab.com/fitmulticell/libpetab-python-](https://gitlab.com/fitmulticell/libpetab-python-MS)
164 **MS**.

165 As imaging data are often processed to obtain informative summary statistics, the FitMul-
166 tiCell pipeline includes a class definition for the construction of summary statistics. Several
167 common summary statistics for imaging data are already provided (see Results section) and
168 customized statistics can be implemented. Furthermore, it is possible to automatically con-
169 struct informative summary statistics [Fearnhead and Prangle, 2012, Schälte and Hasenauer,

170 2022].

171 **2.2.2 Simulation**

172 The FitMultiCell pipeline is designed for the simulation-based analysis of multi-cellular pro-
173 cesses. Accordingly, we allow for simulation of advanced models \mathcal{M} for cells and tissues
174 (using cellular automata and cellular Potts models), extra-cellular concentration fields (us-
175 ing partial differential equations) and intra-cellular dynamics (using ordinary or stochastic
176 differential equations or continuous-time Markov jump processes).

177 The FitMultiCell pipeline implements a comprehensive interface to Morpheus, including pa-
178 rameter mapping and simulation result extraction. This renders the functionalities of Mor-
179 pheus (e.g. model construction, simulation and visualization) as well as features such as a
180 comprehensive GUI for rapid prototyping available within the FitMultiCell pipeline. As
181 Morpheus is broadly applicable, widely used for a variety of biological problems, and compu-
182 tationally efficient (see, e.g., Köhn-Luque et al. [2011], Imle et al. [2019] and Vu et al. [2019]),
183 the tight integration of Morpheus in the FitMultiCell pipeline will be beneficial for users.

184 Additionally, the modular architecture of the FitMultiCell pipeline allows for the interfacing
185 of additional modeling and simulation toolboxes, as well as user-provided simulation codes.

186 **2.2.3 Inference**

187 The FitMultiCell pipeline is designed for simulation-based inference, a class of approaches
188 circumventing the evaluation of the likelihood function. This is important for the study of
189 stochastic multi-cellular processes, but also allows for the application to deterministic models.

190 The FitMultiCell pipeline implements a comprehensive interface to pyABC [Schälte et al.,
191 2022], including parameter and condition mapping for multi-experiment and multi-data type
192 inference. This renders the state-of-the-art Approximate Bayesian Computation Sequential
193 Monte Carlo (ABC-SMC) method easily accessible to users of the FitMultiCell pipeline.
194 ABC-SMC methods approximate the posterior distribution by constructing a sequence of
195 particles which resembles the data (in terms of summary statistics) more and more closely
196 [Toni and Stumpf, 2010]. Well-tested adaptation methods, e.g. for acceptance thresholds,
197 proposal distributions, and population sizes, render pyABC accessible to non-expert users.
198 Furthermore, pyABC allows for exact inference [Schälte and Hasenauer, 2020] and we recently
199 implemented automatic data normalization, summary statistics construction, and measure-
200 ment noise handling to enable the robust estimation of parameters of multi-scale models
201 [Schälte and Hasenauer, 2022, Schälte et al., 2021]. For the combined use of Morpheus and
202 pyABC, we implemented an early rejection mechanism that discards simulations as early as
203 possible, e.g. if they exceed an upper time limit. This makes the analysis robust to unex-

204 pectedly long-running simulations, e.g. due to an excessive number of cells.

205 We provided the interface to pyABC as this tool has been successfully used in a broad
206 spectrum of applications, e.g., cardiac electrophysiology [Cantwell et al., 2019], human atrial
207 cells [Houston et al., 2020], cancer [Colom et al., 2021], gene expression [Coulier et al., 2021],
208 universe expansion [Bernardo and Said, 2021], and bee colonies [Minucci et al., 2021]. This
209 underlines its applicability to a broad spectrum of inference tasks for multi-cellular processes.
210 Additionally, the modular architecture of the FitMultiCell pipeline allows for the interfacing
211 of additional inference tools, as well as user-provided inference algorithms.

212 2.2.4 Distributed execution

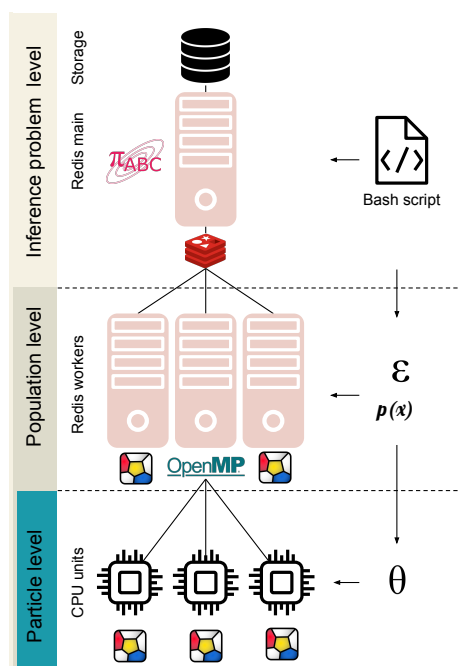


Figure 2: Illustration of the parallel framework of FitMultiCell. **Inference level:** A main process manages the pyABC analysis workflow and SQL data storage. **Population level:** In each ABC-SMC generation, the main process delegates to a number of distributed worker processes the task of sampling parameters (from proposal distributions $p(x)$) and synthetic data sets, until sufficiently many fulfil the generation-specific acceptance criterion (such as the acceptance thresholds \mathcal{E}). Work distribution, communication, and storage of intermediate results across various computational nodes and processing units are managed via a central Redis server. **Particle level:** Each single simulation of synthetic data (or groups of simulations for related perturbation scenarios in a multi-experiment setting) is performed using Morpheus, optionally with shared-memory parallelization via OpenMP.

213 Parameter estimation often requires thousands to millions of stochastic model simulations,

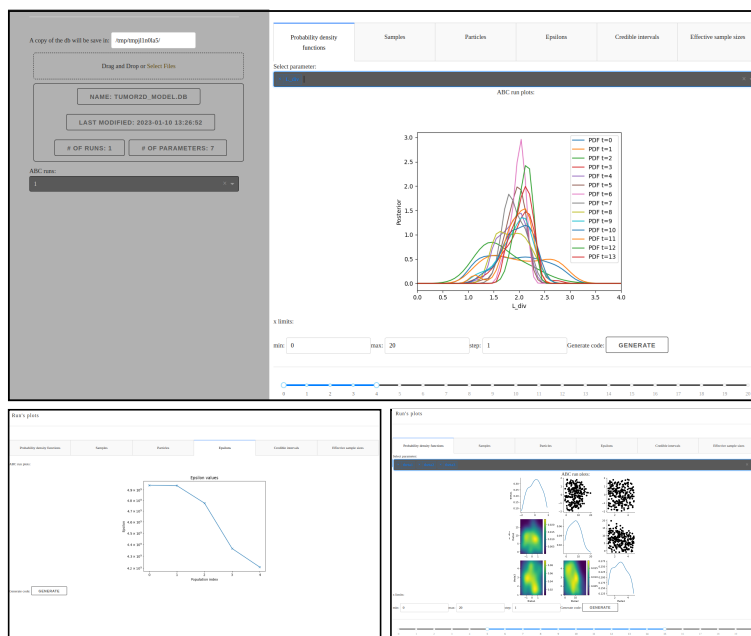


Figure 3: Several screenshots of the visualization and diagnostics GUI.

214 which is computationally demanding for complex multi-cellular processes. Distributed exe-
 215 cution of the computational tasks is thus paramount (Figure 2). Within the FitMultiCell
 216 pipeline, parallelization can happen on three levels to efficiently exploit high-performance
 217 computing (HPC) infrastructure:

- 218 • *Individual simulations* can be parallelized within the employed simulation toolbox.
 219 Morpheus supports the use of multiple threads using OpenMP. In addition to ODEs
 220 and PDEs, Morpheus also provides a parallel and exact solver for CPMs.
- 221 • *Individual summary statistics evaluations* can be parallelized within the FitMultiCell
 222 pipeline if multiple individual simulations are required. This is for instance the case if
 223 experimental replicates are available for stochastic processes and multiple experimental
 224 conditions are considered. As the respective simulations are independent, they can be
 225 trivially parallelized across multiple threads.
- 226 • *Parameter estimation* can be parallelized within the employed parameter estimation
 227 toolbox. PyABC supports single-machine multi-core execution and multi-machine dis-
 228 tributed execution. A main process manages the communication across SMC gener-
 229 ations and post-processing of accepted particle populations, while the computa-
 230 tion-heavy simulations and summary statistic evaluations are delegated to a set of parallel
 231 worker processes (see Figure 2). pyABC provides two parallelization strategies, static
 232 and dynamic scheduling, which distribute work across computational resources, aiming
 233 to minimize the overall CPU time, or the overall wall time, respectively [Klinger et al.,

234 2018].

235 To facilitate the setup of the required server-worker architecture, the FitMultiCell pipeline
236 comes with bash scripts that handle the resource allocation and communication between
237 nodes, and which can be used to run the pipeline on HPC clusters with minimum code
238 modification. While parallelization is available at multiple levels, the most efficient resource
239 use will often be achieved by dedicating many workers to the particle population and setting
240 Morpheus to single-threaded simulation mode.

241 **2.2.5 Analysis and visualization**

242 The FitMultiCell pipeline provides a GUI for the analysis of the parameter estimation results.
243 This GUI can load the shareable SQL database generated by pyABC, but is flexible enough
244 to visualize the results for other sampling tools after the result files were reformatted. Among
245 other things, the GUI allows for the visualization of (1) samples using uni- and bi-variate
246 plots, (2) sampling diagnostics like the decrease of the acceptance threshold over generations,
247 and (3) the ability to generate the code for any plot that is generated.

248 **2.3 Implementation and development**

249 The FitMultiCell pipeline is written in Python and available on GitLab ([https://gitlab.com/](https://gitlab.com/fitmulticell/fit)
250 [fitmulticell/fit](https://gitlab.com/fitmulticell/fit)) and Zenodo (<https://doi.org/10.5281/zenodo.7646287>) under a BSD-3-
251 Clause license. It is being developed by contributors from three institutions and others are
252 invited to contribute. Code quality is monitored via unit tests and continuous integration.
253 The tool can be installed from the Python Package Index (PyPI). Detailed documentation
254 of the FitMultiCell platform is available at <https://fitmulticell.readthedocs.io>, which
255 covers installation, setting up the modeling and estimation problem, and running the param-
256 eter estimation process, including on HPC and cloud infrastructures.

257 To ensure ease of use, FitMultiCell pipeline integrates currently only tools which are easy to
258 install and available under permissive licenses:

- 259 • Morpheus is available as a git repository (<https://gitlab.com/morpheus.lab/morpheus>)
260 under the BSD-3-Clause license. It is written in C++ and available for all major oper-
261 ating systems as pre-compiled packages together with training materials and a model
262 repository at (<https://morpheus.gitlab.io/>).
- 263 • pyABC is hosted on GitHub (<https://github.com/icb-dcm/pyabc>) under the BSD-
264 3-Clause license. It is written in Python and can be installed directly via (PyPI). Its
265 many features are documented at (<https://pyabc.readthedocs.io>).

266 **3 Results**

267 To assess the performance of the FitMultiCell pipeline, we evaluated it using a broad spec-
268 trum of test and application examples. In the following, we present its core properties
269 for a few selected models of multi-cellular processes. Several other applications to various
270 multi-cellular problems and different data types have been published separately and are not
271 included here (See Boutillon et al. [2022] Bundgaard et al. [2022]).

272 All the following results were obtained on the JUWELS standard compute nodes of the Su-
273 percomputing Center in Jülich, Germany. Details on the technical specifications are provided
274 in the Supplementary Material.

275 **3.1 Standards supported by FitMultiCell pipeline allow for re-** 276 **implementation of published application problems**

277 The FitMultiCell pipeline allows for the standardized description of models, datasets and
278 parameter estimation problems. To ensure that the supported standards are practically
279 useful, we assessed to which degree we can implement already published application problems.

280 We considered three applications capturing different biological and technical problems: (M1)
281 a model of virus transmission via cell-free virions and cell-to-cell contact [Kumberger et al.,
282 2018]; (M2) a model of tumor spheroid growth [Jagiella et al., 2017]; and (M3) a model de-
283 scribing the mechano-sensing of the metabolic status during liver regeneration [Meyer et al.,
284 2020]. The models M1 and M2 were originally not available in MorpheusML and were re-
285 implemented for the purpose of this study, while M3 was already published in MorpheusML.
286 For all applications, we created the P_Etab-MS description of the parameter estimation prob-
287 lems. Details on the application problems are provided below and in the Supplementary
288 Material.

289 We compared the implementation of the models in MorpheusML with the originally published
290 models and found a good resemblance. Furthermore, P_Etab-MS was flexible enough to
291 describe all parameter estimation problems. This suggests that the standards employed in
292 the FitMultiCell pipeline are sufficient for a broad spectrum of applications.

293 **3.2 Parallelization in FitMultiCell pipeline provides substantial** 294 **wall-time reduction**

295 As the efficient use of computing resources is of crucial importance for parameter estimation,
296 we evaluated the parallel efficiency achieved using the FitMultiCell pipeline. We considered
297 a model of the spread of a viral infection within a tissue distinguishing between virus trans-

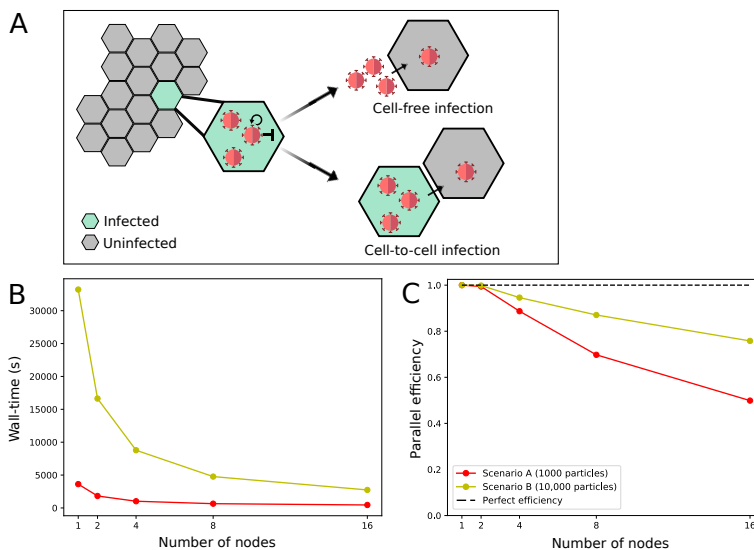


Figure 4: Performance of the parallelized FitMultiCell pipeline. (A) Illustration of the used model M1 for viral transmission within the host tissue. (B) Wall-time of two different fit scenarios across different numbers of used compute nodes, each consisting of 48 CPU cores. (C) Parallel efficiency of the FitMultiCell pipeline. The dashed line indicates perfect efficiency, i.e. a wall-time directly inversely proportional to the number of nodes, compared to single-node execution. For each choice of nodes, three consecutive ABC-SMC generations were run, with population sizes of $N = 1,000$ (Scenario A) and $N = 10,000$ (Scenario B).

298 mission via cell-free virions and direct cell-to-cell contact [Kumberger et al., 2018] (Figure 4A
 299 and Supplementary Material, Section 4).

300 In the FitMultiCell pipeline, parallelization is available within and across individual simu-
 301 lation particles. For the considered problems, we parallelize exclusively on the population
 302 level to provide the most efficient resource usage; however, this may depend on the specific
 303 problem.

304 To assess the parallel efficiency, we performed parameter estimation using the ABC-SMC
 305 algorithm implemented in pyABC with the dynamic scheduling option. The algorithms were
 306 run for three generations with two different population sizes: (Scenario A) 1,000 particles;
 307 and (Scenario B) 10,000 particles. As higher population sizes improve the posterior approxi-
 308 mation but are computationally more demanding, both scenarios are relevant. We performed
 309 this task using 1, 2, 4, 8 and 16 compute nodes, each consisting of 48 CPU cores.

For both Scenarios A and B, we observed a substantial reduction in wall-time when using
 higher numbers of nodes, to a fraction of the single-node execution wall-time which already
 used 48 CPU cores (Figure 4B). Yet, the parallel efficiency (PE), dropped (Figure 4C) – for
 the case

$$PE = \frac{\{\text{wall-time for run on single compute node}\}}{\{\text{wall-time for run on } i \text{ compute nodes}\} \cdot i},$$

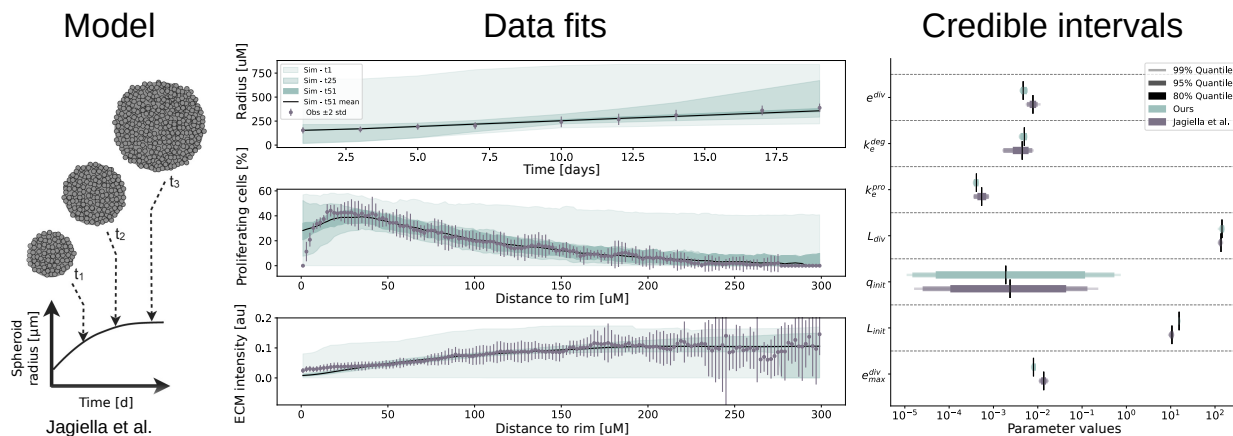


Figure 5: Result of FitMultiCell pipeline for the model of tumor spheroid growth. Illustration of the model (Left). Experimental data (gray) and simulation results (green) (middle). For the simulations associated with different generations the interval between the 2.5th and the 97.5th percentile are shown. Credible interval for 7 estimated parameters obtained using the original implementation [Jagiella et al., 2017] (gray) and the FitMultiCell pipeline (green) (right).

310 for the case of 16 nodes (768 cores), we found in Scenario A a parallel efficiency of 49%
 311 and in Scenario B a parallel efficiency of 75%. The higher parallel efficiency in Scenario B
 312 is plausible as individual generations require more time, which reduces the contributions of
 313 the tails of generations in which idle times occur due to differences in computation times for
 314 individual particles (see also Klinger et al. [2018]).

315 In summary, our evaluation confirmed an overall good scaling of the FitMultiCell pipeline,
 316 yielding a wall-time reduction of several ten-fold compared to a single-node execution and
 317 several hundred-fold compared to single-core execution. As the number of proposed particles
 318 required to generate a specific number of accepted particles increases over generations, the
 319 parallel efficiency for production runs with the usual 15 to 40 generations should be higher
 320 than what has been observed here.

321 **3.3 FitMultiCell pipeline facilitates the study of heterogeneous** 322 **datasets via automatically tuned algorithms**

323 To assess the benefit of the tight integration of modeling and parameter estimation tools in
 324 the FitMultiCell pipeline, and the availability of advanced inference algorithms, we considered
 325 the model of tumor spheroid growth [Jagiella et al., 2017] (Figure 5(left)). The original model
 326 was used to study growth control mechanisms and the effect of nutrient supply [Jagiella et al.,

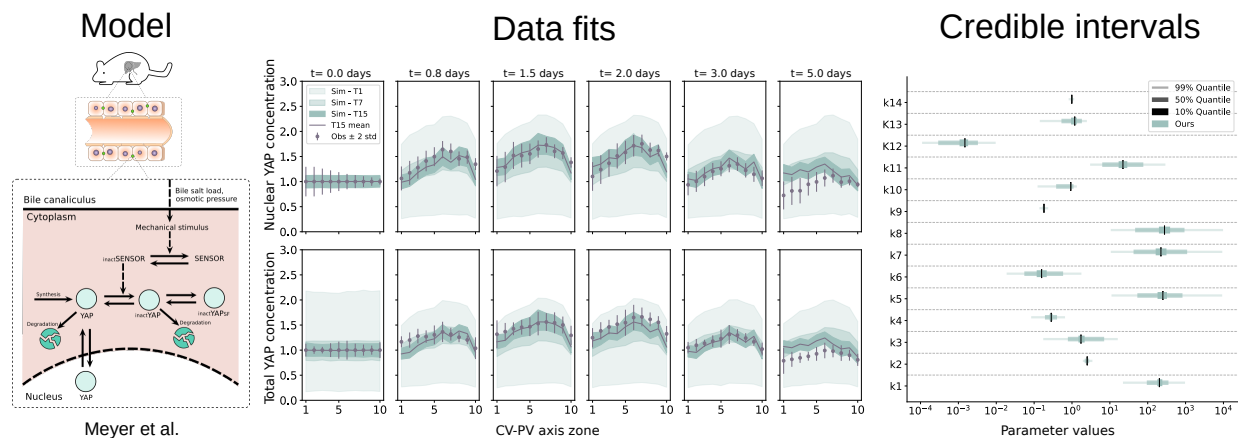


Figure 6: Result of FitMultiCell pipeline for the model of mechano-sensing of the metabolic status during liver regeneration. Illustration of the model (left). Experimental data (gray) and simulation results (green) for different combinations of tissue location (from 1-10) and time point (t0-t5.0 days) (middle). For the simulations associated with different generations the interval between the 2.5th and the 97.5th percentile are shown. Credible interval for 14 estimated parameters (right).

327 2016, 2017]. Yet, the source code of this multi-cellular model entangled with its simulator
 328 is highly specific and no longer maintained, complicating the use of this model in further
 329 studies.

330 We implemented the model in MorpheusML and made it available through a public model
 331 repository (<https://identifiers.org/morpheus/M0007>). The cell population was described
 332 using a stochastic CPM which accounts for cell division and death as well as cell-cell inter-
 333 actions, while the concentrations of extracellular substances were described using partial
 334 differential equations (PDEs). The estimation problem for the seven unknown parameters
 335 was encoded using PETA-MS. We considered all available datasets: a time-course for the tu-
 336 mor spheroid radius determined by bright field microscopy; and snapshots for radial profiles
 337 of markers for proliferating cells as well as extra-cellular matrix abundance determined from
 338 fluorescence microscopy.

339 In our previous publication considering the parameter estimation problem [Jagiella et al.,
 340 2017], we manually defined weights to quantify the relative importance of different sum-
 341 mary statistics for the heterogeneous dataset. As this was a time-consuming process, here
 342 we employed a fully automatic approach for summary statistics weighting based on inverse
 343 regression (see Supplementary Material, Section 2 for details), which is available via the Fit-
 344 MultiCell pipeline. The specification of the parameter estimation task does only require a
 345 few lines of Python code given MorpheusML and PETA-MS files.

346 We ran the ABC-SMC algorithm with a population size of 500 particles and set as stopping
347 condition a maximum wall-time of 48h, within which the pipeline was able to finish 46
348 generations. The comparison of simulated and observed summary statistics showed that the
349 model is able to fit the data accurately, with substantially improving fit quality in later
350 ABC-SMC generations (Figure 5 (middle)). Exception are, similar to the original model,
351 the fraction of proliferating cells and the ECM density at small distances to the rim, which
352 the model over- and underestimates, respectively, in correspondence to the original analysis
353 [Jagiella et al., 2017], indicating that the model needs to be refined in this regard. The analysis
354 of credible intervals reveals that with the exception of the initial fraction of quiescent cells
355 c_{init} , all parameters are identifiable with small uncertainties. The parameter estimates and
356 uncertainty intervals obtained using our model are in excellent agreement with those in the
357 original analysis (Figure 5(right)). Hence, the FitMultiCell pipeline was able to reproduce the
358 original results, while simplifying implementation and reducing the need for manual tuning.

359 **3.4 FitMultiCell pipeline facilitates parameter estimation for new** 360 **applications**

361 The parameters of multi-scale processes are often still adapted manually, e.g. due to the
362 difficulty of setting up proper parameter estimation and its computational cost. As this
363 involves manual work, it can lead to non-reproducible results and does not provide any
364 information about parameter uncertainties. We assessed whether the FitMultiCell pipeline
365 can easily replace manual parameter tuning. We studied a model describing the mechano-
366 sensing of the metabolic status during liver regeneration after partial hepatectomy in mice,
367 simulating the reaction network dynamics in hepatocytes along the central-portal axis of a
368 liver lobule by a spatial array of coupled ODEs with spatially heterogeneous inputs [Meyer
369 et al., 2020]. For this model, the parameters were previously determined manually using
370 data for two observables: the concentration of the YAP protein in the nucleus of hepatocytes
371 (NYAP), and the total concentration of YAP protein in hepatocytes (TYAP), see Figure 6
372 (left).

373 The model was already implemented in MorpheusML and is available from a public model
374 repository (<https://identifiers.org/morpheus/M7990>). Yet, in exchange with the au-
375 thors of the original publication, we decided (1) to relax the quasi-steady-state assumption
376 of the intracellular dynamics and performed a full spatio-temporal simulation, (2) to extend
377 the biochemical model by an observer model of the microscopy setup that introduces addi-
378 tional scaling parameters between protein concentration and observed fluorescence intensity,
379 and (3) to account for the measurement noise. Complementary, we created the PETab-MS
380 files encoding the estimation problem for the 14 unknown parameters. Previously, due to
381 the employed quasi-steady-state assumption, only the ratios of forward and backward rate

382 constants were identifiable.

383 We ran the ABC-SMC inference with a population size of 1,000 particles and a wall-time
384 limit of 24h. To save computational resources, we employed an early rejection strategy
385 to reject particles based on a maximum runtime of 15min for individual simulations not
386 matching the data. The simulated trajectories in later generations of the inference process
387 fitted the data for TYAP and NYAP mostly well (Figure 6 (middle)). An exception were
388 the pericentral locations (CV-PV zones 1-5) at the last time point $t = 5.0days$, where the
389 simulations couldn't match the low concentrations present in the data, hinting at a transition
390 to homeostasis and a time-dependence of some parameters over longer time scales of many
391 days. The credible intervals indicate that all 14 parameters are identifiable (Figure 6 (right)).
392 Interestingly, the parameter describing the fluorescence intensity normalization (k_{14}) was
393 estimated close to one, which supports the hypothesis that both microscopy-based observables
394 can be treated with the same normalization [Meyer et al., 2020]. Moreover, the ratios of
395 rate constants for reversible reactions were found to be on the same order of magnitude
396 as estimated using the quasi-steady state assumption in [Meyer et al., 2020]. Hence, our
397 study underpinned previous conclusions [Meyer et al., 2020], but also demonstrated that
398 the FitMultiCell pipeline allows directly for an uncertainty-aware study of multi-cellular
399 processes.

400 4 Discussion

401 Quantitative data-based modeling of multi-cellular processes is challenging, because the mod-
402 els are often stochastic and computationally demanding. Furthermore, due to a lack of
403 standards, the reusability of codes and pipelines is limited. Motivated by these issues, we
404 developed the FitMultiCell pipeline, which covers the entire workflow of model development,
405 simulation, and systematic parameter inference (on HPC or cloud infrastructures) based on
406 standardized input formats. Thereby, it contributes to the accelerated testing of biological
407 hypotheses.

408 We used the FitMultiCell pipeline to study various application problems. This demonstrated
409 that the proposed pipeline is widely applicable and can recover and confirm previous results.
410 Further, we showed that it can replace manual parameter tuning, thus accelerating and
411 solidifying the quantitative modeling of multi-cellular processes. Its modular implementation
412 scales to HPC infrastructures and thereby facilitates inference for computationally expensive
413 problems.

414 While the FitMultiCell pipeline already provides the necessary features, there are multiple
415 directions in which it can be developed further. (1) Statistical inference for computationally
416 expensive models can become challenging even when using massive parallelization. To address

417 this, the use of cheaper surrogate models could be investigated for guiding parameter search
418 and reducing the number of model simulations [Prangle, 2016, Prescott and Baker, 2021].
419 Furthermore, one could make use of the idle time at the end of generations, e.g. by pre-
420 sampling the next generation and subsequently correcting for bias. (2) Methods for the
421 automatic construction of summary statistics need to be explored. While it is possible to
422 construct summary statistics semi-automatically [Blum et al., 2013] for the type of image data
423 frequently accompanying models of multi-cellular processes, automatic construction based on
424 machine learning approaches, more specifically convolutional networks with prior information
425 gained from transfer learning, could substantially improve statistics quality at decreased
426 training cost. (3) Extension of the FitMultiCell pipeline to additional modeling, simulation
427 and parameter estimation frameworks will increase its applicability. While Morpheus and
428 pyABC cover already a wide range of applications, an integration of further simulation tools
429 (e.g. Ghaffarizadeh et al. [2018], Merks et al. [2011], Mirams et al. [2013], Swat et al. [2012])
430 and inference tools (e.g. Dutta et al. [2017], Kangasrääsiö et al. [2016]) could facilitate the
431 use of complementary methods and thus grow the application spectrum further.

432 In conclusion, we illustrated that standardized workflows for the quantitative modeling of
433 multi-cellular processes are feasible. The FitMultiCell pipeline and the standard PTab-
434 MS provide starting points for further development. Already in its current form, a broad
435 spectrum of projects can profit from them to achieve systematic and scalable inference of
436 unknown parameters.

437 **Acknowledgements**

438 We acknowledge fruitful discussions with colleagues at Morpheus.lab and the Gauss Centre
439 for Supercomputing e.V. (www.gauss-centre.eu) for providing computing time on the GCS
440 Supercomputer JUWELS [Jülich Supercomputing Centre, 2019] at Jülich Supercomputing
441 Centre (JSC).

442 **Funding**

443 This work was supported by the German Federal Ministry of Education and Research (BMBF)
444 (FitMultiCell/031L0159C and EMUNE/031L0293C). JH acknowledges support by the Ger-
445 man Research Foundation (DFG) under Germany's Excellence Strategy (EXC 2047 390873048
446 and EXC 2151 390685813) and via the Schlegel Professorship for JH. FG was additionally
447 supported by the Chica and Heinz Schaller Foundation. YS acknowledges financial support
448 by the German Research Foundation (DFG) (Metaflammation: SFB 1454 - 432325352) and
449 the Joachim Herz Stiftung. LB was supported by the BMBF (LiSyM-Cancer/031L0258A).

450 References

- 451 A. R. A. Anderson and V. Quaranta. Integrative mathematical oncology. *Nat. Rev. Cancer*, 8(3):227–234, Mar. 2008.
- 452 A. C. Babbie and M. P. H. Stumpf. How to deal with parameters for whole-cell modelling. *J. R. Soc. Interface*, 14(133), 2017. ISSN
453 1742-5689. doi: 10.1098/rsif.2017.0237. URL <http://rsif.royalsocietypublishing.org/content/14/133/20170237>.
- 454 M. A. Beaumont, W. Zhang, and D. J. Balding. Approximate Bayesian Computation in Population Genetics. *Genetics*, 162(4):
455 2025–2035, 12 2002.
- 456 R. C. Bernardo and J. L. Said. Towards a model-independent reconstruction approach for late-time hubble data. *J. Cosmol. Astropart.*
457 *Phys.*, 2021(08):027, 2021.
- 458 M. G. Blum, M. A. Nunes, D. Prangle, and S. A. Sisson. A comparative review of dimension reduction methods in approximate Bayesian
459 computation. *Stat. Sci.*, 28(2):189–208, 2013.
- 460 A. Boutillon, S. Escot, A. Elouin, D. Jahn, S. González-Tirado, J. Starrau, L. Bruschi, and N. B. David. Guidance by followers
461 ensures long-range coordination of cell migration through α -catenin mechanoperception. *Dev. Cell*, 57(12):1529–1544.e5, 2022. doi:
462 10.1016/j.devcel.2022.05.001.
- 463 N. Bundgaard, C. Harmel, A. Imle, S. Sid Ahmed, B. Frey, J. Starrau, O. T. Fackler, and F. Graw. Inferring cell motility in complex
464 environments with incomplete tracking data. *bioRxiv*, 2022. doi: 10.1101/2022.02.10.479738. URL [https://www.biorxiv.org/content/](https://www.biorxiv.org/content/early/2022/02/10/2022.02.10.479738)
465 [early/2022/02/10/2022.02.10.479738](https://www.biorxiv.org/content/early/2022/02/10/2022.02.10.479738).
- 466 C. D. Cantwell, Y. Mohamied, K. N. Tzortzis, S. Garasto, C. Houston, R. A. Chowdhury, F. S. Ng, A. A. Bharath, and N. S.
467 Peters. Rethinking multiscale cardiac electrophysiology with machine learning and predictive modelling. *Computers in Bi-*
468 *ology and Medicine*, 104:339 – 351, 2019. ISSN 0010-4825. doi: <https://doi.org/10.1016/j.compbimed.2018.10.015>. URL
469 <http://www.sciencedirect.com/science/article/pii/S0010482518303147>.
- 470 B. Colom, A. Herms, M. Hall, S. Dentre, C. King, R. Sood, M. Alcolea, G. Piedrafita, D. Fernandez-Antoran, S. Ong, et al. Mutant
471 clones in normal epithelium outcompete and eliminate emerging tumours. *Nature*, 598(7881):510–514, 2021.
- 472 A. Coulier, S. Hellander, and A. Hellander. A multiscale compartment-based model of stochastic gene regulatory networks using
473 hitting-time analysis. *J. Chem. Phys.*, 154(18):184105, 2021.
- 474 K. Durso-Cain, P. Kumberger, Y. Schälte, T. Fink, H. Dahari, J. Hasenauer, S. L. Uprichard, and F. Graw. HCV spread kinetics
475 reveal varying contributions of transmission modes to infection dynamics. *Viruses*, 13(7), July 2021. ISSN 1999-4915. doi: 10.3390/
476 v13071308.
- 477 R. Dutta, M. Schoengens, J.-P. Onnela, and A. Mira. Abcpy: A user-friendly, extensible, and parallel library for approximate Bayesian
478 computation. In *Proceedings of the Platform for Advanced Scientific Computing Conference, PASC '17*, pages 8:1–8:9, New York,
479 NY, USA, 2017. ACM. ISBN 978-1-4503-5062-4. doi: 10.1145/3093172.3093233.
- 480 P. Fearnhead and D. Prangle. Constructing summary statistics for approximate Bayesian computation: semi-automatic approximate
481 Bayesian computation. *J. R. Stat. Soc. B*, 74(3):419–474, 2012.
- 482 A. G. Fletcher and J. M. Osborne. Seven challenges in the multiscale modeling of multicellular tissues. *WIREs Mechanisms of Disease*,
483 14(1):e1527, 2022. doi: <https://doi.org/10.1002/wsbm.1527>. URL <https://wires.onlinelibrary.wiley.com/doi/abs/10.1002/wsbm.1527>.
- 484 A. Ghaffarizadeh, R. Heiland, S. H. Friedman, S. M. Mumenthaler, and P. Macklin. Physicell: An open source physics-based cell
485 simulator for 3-d multicellular systems. *PLoS Comput. Biol.*, 14(2):e1005991, Feb 2018. doi: 10.1371/journal.pcbi.1005991.
- 486 J. Hasenauer, N. Jagiella, S. Hross, and F. J. Theis. Data-driven modelling of biological multi-scale processes. *J. Coupled Syst.*
487 *Multiscale Dyn.*, 3(2):101–121, 9 2015.
- 488 C. Houston, B. Marchand, L. Engelbert, and C. D. Cantwell. Reducing complexity and unidentifiability when modelling human
489 atrial cells. *Philos. Trans. A Math. Phys. Eng. Sci.*, 378(2173):20190339, 2020. doi: 10.1098/rsta.2019.0339. URL [https://](https://royalsocietypublishing.org/doi/abs/10.1098/rsta.2019.0339)
490 royalsocietypublishing.org/doi/abs/10.1098/rsta.2019.0339.
- 491 A. Imle, P. Kumberger, N. D. Schnellbacher, J. Fehr, P. Carrillo-Bustamante, J. Ales, P. Schmidt, C. Ritter, W. J. Godinez, B. Müller,
492 et al. Experimental and computational analyses reveal that environmental restrictions shape HIV-1 spread in 3D cultures. *Nat.*
493 *Commun.*, 10(1):2144, 2019.

- 494 N. Jagiella, B. Müller, M. Müller, I. E. Vignon-Clementel, and D. Drasdo. Inferring growth control mechanisms in growing multi-cellular
495 spheroids of NSCLC cells from spatial-temporal image data. *PLoS Comput. Biol.*, 12(2):e1004412, Feb. 2016. doi: 10.1371/journal.
496 pcbi.1004412.
- 497 N. Jagiella, D. Rickert, F. J. Theis, and J. Hasenauer. Parallelization and high-performance computing enables automated statistical
498 inference of multi-scale models. *Cell Syst.*, 4(2):194–206, 02 2017.
- 499 S. T. Johnston, M. J. Simpson, D. L. McElwain, B. J. Binder, and J. V. Ross. Interpreting scratch assays using pair density dynamics
500 and approximate Bayesian computation. *Open Biol.*, 4(9):140097, Sept. 2014. doi: 10.1098/rsob.140097.
- 501 A. Kangasräsiö, J. Lintusaari, K. Skytén, M. Järvenpää, H. Vuollekoski, M. Gutmann, A. Vehtari, J. Corander, and S. Kaski. ELFI:
502 Engine for Likelihood-Free Inference. In *NIPS 2016 Workshop on Advances in Approximate Bayesian Inference*, 2016.
- 503 R. A. Kerr, T. M. Bartol, B. Kaminsky, M. Ditttrich, J.-C. J. Chang, S. B. Baden, T. J. Sejnowski, and J. R. Stiles. Fast monte carlo
504 simulation methods for biological reaction-diffusion systems in solution and on surfaces. *SIAM J. Sci. Comput.*, 30(6):3126–3149,
505 2008.
- 506 E. Klinger, D. Rickert, and J. Hasenauer. pyABC: distributed, likelihood-free inference. *Bioinf.*, 34(20):3591–3593, 10 2018.
- 507 A. Köhn-Luque, W. de Back, J. Starruß, A. Mattiotti, A. Deutsch, J. M. Pérez-Pomares, and M. A. Herrero. Early embryonic vascular
508 patterning by matrix-mediated paracrine signalling: A mathematical model study. *PLoS ONE*, 6(9):1–12, 09 2011. doi: 10.1371/
509 journal.pone.0024175. URL <https://doi.org/10.1371/journal.pone.0024175>.
- 510 P. Kumberger, K. Durso-Cain, S. Uprichard, H. Dahari, and F. Graw. Accounting for space—quantification of cell-to-cell transmission
511 kinetics using virus dynamics models. *Viruses*, 10(4):200, Apr 2018. ISSN 1999-4915. doi: 10.3390/v10040200. URL <http://dx.doi.org/10.3390/v10040200>.
- 513 S. M. Lewis, M.-L. Asselin-Labat, Q. Nguyen, J. Berthelet, X. Tan, V. C. Wimmer, D. Merino, K. L. Rogers, and S. H. Naik. Spatial
514 omics and multiplexed imaging to explore cancer biology. *Nat. Methods*, 18(9):997–1012, 2021.
- 515 A. L. MacLean, S. Filippi, and M. P. H. Stumpf. The ecology in the hematopoietic stem cell niche determines the clinical outcome in
516 chronic myeloid leukemia. *Proc. Natl. Acad. Sci. USA*, Jan. 2014. doi: pnas.1317072111.
- 517 R. M. Merks, M. Guravage, D. Inzé, and G. T. Beemster. Virtualleaf: an open-source framework for cell-based modeling of plant tissue
518 growth and development. *Plant Physiol.*, 155(2):656–666, 2011.
- 519 K. Meyer, H. Morales-Navarrete, S. Seifert, M. Wilsch-Braeuninger, U. Dahmen, E. M. Tanaka, L. Bruschi, Y. Kalaidzidis, and M. Zerial.
520 Bile canaliculi remodeling activates yap via the actin cytoskeleton during liver regeneration. *Mol. Syst. Biol.*, 16(2):e8985, 2020.
- 521 J. M. Minucci, R. Curry, G. DeGrandi-Hoffman, C. Douglass, K. Garber, and S. T. Purucker. Inferring pesticide toxicity to honey bees
522 from a field-based feeding study using a colony model and bayesian inference. *Ecol. Appl.*, 31(8):e02442, 2021.
- 523 G. R. Mirams, C. J. Arthurs, M. O. Bernabeu, R. Bordas, J. Cooper, A. Corrias, Y. Davit, S.-J. Dunn, A. Fletcher, D. Harvey, M. Marsh,
524 J. Osborne, P. Pathmanathan, J. Pitt-Francis, J. Southern, N. Zenzemi, and D. Gavaghan. Chaste: an open source C++ library
525 for computational physiology and biology. *PLoS Comput. Biol.*, 9(3):e1002970, Mar. 2013. doi: 10.1371/journal.pcbi.1002970.
- 526 D. Prangle. Lazy ABC. *Stat. Comput.*, 26(1):171–185, 2016.
- 527 T. P. Prescott and R. E. Baker. Multifidelity approximate Bayesian computation with sequential Monte Carlo parameter sampling.
528 *SIAM-ASA J. Uncertain. Quantif.*, 9(2):788–817, 2021.
- 529 J. K. Pritchard, M. T. Seielstad, A. Perez-Lezaun, and M. W. Feldman. Population growth of human y chromosomes: a study of y
530 chromosome microsatellites. *Mol. Biol. Evol.*, 16(12):1791–1798, 1999.
- 531 P. Richmond, D. Walker, S. Coakley, and D. Romano. High performance cellular level agent-based simulation with FLAME for the
532 GPU. *Brief Bioinform.*, 11(3):334–347, Feb. 2010. doi: 10.1093/bib/bbp073.
- 533 Y. Schälte and J. Hasenauer. Efficient exact inference for dynamical systems with noisy measurements using sequential approximate
534 Bayesian computation. *Bioinf.*, 36(Supplement 1):i551–i559, 7 2020. ISSN 1367-4803. doi: 10.1093/bioinformatics/btaa397.
- 535 Y. Schälte and J. Hasenauer. Informative and adaptive distances and summary statistics in sequential approximate Bayesian computa-
536 tion. *bioRxiv*, 2022. doi: 10.1101/2022.03.18.484896. URL <https://www.biorxiv.org/content/early/2022/03/20/2022.03.18.484896.1>.

- 537 Y. Schälte, E. Alamoudi, and J. Hasenauer. Robust adaptive distance functions for approximate Bayesian inference on outlier-corrupted
538 data. *bioRxiv*, 2021.
- 539 L. Schmiester, Y. Schälte, F. T. Bergmann, T. Camba, E. Dudkin, J. Egert, F. Fröhlich, L. Fuhrmann, A. L. Hauber, S. Kemmer,
540 P. Lakrisenko, C. Loos, S. Merkt, W. Müller, D. Pathirana, E. Raimúndez, L. Refisch, M. Rosenblatt, P. L. Stapor, P. Städter,
541 D. Wang, F.-G. Wieland, J. R. Banga, J. Timmer, A. F. Villaverde, S. Sahle, C. Kreutz, J. Hasenauer, and D. Weindl. PETA—
542 interoperable specification of parameter estimation problems in systems biology. *PLoS Comput. Biol.*, 17(1):1–10, January 2021.
543 doi: 10.1371/journal.pcbi.1008646.
- 544 Y. Schälte, E. Klinger, E. Alamoudi, and J. Hasenauer. pyabc: Efficient and robust easy-to-use approximate bayesian computation. *J.*
545 *Open Source Softw.*, 7(74):4304, 2022. doi: 10.21105/joss.04304. URL <https://doi.org/10.21105/joss.04304>.
- 546 S. A. Sisson, Y. Fan, and M. Beaumont. *Handbook of approximate Bayesian computation*. Chapman and Hall/CRC, 2018.
- 547 A. Sottoriva, H. Kang, Z. Ma, T. A. Graham, M. P. Salomon, J. Zhao, P. Marjoram, K. Siegmund, M. F. P. D. Shibata, and C. Curtis.
548 A Big Bang model of human colorectal tumor growth. *Nat. Gen.*, 47(3):209–216, Mar. 2015. doi: 10.1038/ng.3214.
- 549 J. Starruß, W. de Back, L. Brusch, and A. Deutsch. Morpheus: A user-friendly modeling environment for multiscale and multicellular
550 systems biology. *Bioinf.*, 30(9):1331–1332, Jan. 2014. doi: 10.1093/bioinformatics/btt772.
- 551 M. H. Swat, G. L. Thomas, J. M. Belmonte, A. Shirinifard, D. Hmeljak, and J. A. Glazier. Multi-scale modeling of tissues using
552 CompuCell3D. *Methods Cell Biol.*, 110:325–366, 2012. doi: 10.1016/B978-0-12-388403-9.00013-8.
- 553 T. Toni and M. P. H. Stumpf. Simulation-based model selection for dynamical systems in systems and population biology. *Bioinf.*, 26
554 (1):104–110, 10 2010.
- 555 T. Toni, G. Jovanovic, M. Huvet, M. Buck, and M. P. H. Stumpf. From qualitative data to quantitative models: analysis of the phage
556 shock protein stress response in Escherichia coli. *BMC Syst. Biol.*, 5(69), May 2011.
- 557 H. T.-K. Vu, S. Mansour, M. Kücken, C. Blasse, C. Basquin, J. Azimzadeh, E. W. Myers, L. Brusch, and J. C. Rink. Dynamic polarization
558 of the multiciliated planarian epidermis between body plan landmarks. *Dev. Cell*, 51(4):526 – 542.e6, 2019. ISSN 1534-5807. doi:
559 <https://doi.org/10.1016/j.devcel.2019.10.022>. URL <http://www.sciencedirect.com/science/article/pii/S153458071930869X>.
- 560 B. Waclaw, I. Bozic, M. E. Pittman, R. H. Hruban, B. Vogelstein, and M. A. Nowak. A spatial model predicts that dispersal and cell
561 turnover limit intratumour heterogeneity. *Nature*, 525(7568):261–264, Aug. 2015. doi: 10.1038/nature14971.
- 562 M. D. Wilkinson, M. Dumontier, I. J. J. Aalbersberg, G. Appleton, M. Axton, A. Baak, N. Blomberg, J.-W. Boiten, L. B. da Silva Santos,
563 P. E. Bourne, J. Bouwman, A. J. Brookes, T. Clark, M. Crosas, I. Dillo, O. Dumon, S. Edmunds, C. T. Evelo, R. Finkers, A. Gonzalez-
564 Beltran, A. J. G. Gray, P. Groth, C. Goble, J. S. Grethe, J. Heringa, P. A. C. 't Hoen, R. Hooft, T. Kuhn, R. Kok, J. Kok, S. J.
565 Lusher, M. E. Martone, A. Mons, A. L. Packer, B. Persson, P. Rocca-Serra, M. Roos, R. van Schaik, S.-A. Sansone, E. Schultes,
566 T. Sengstag, T. Slater, G. Strawn, M. A. Swertz, M. Thompson, J. van der Lei, E. van Mulligen, J. Velterop, A. Waagmeester,
567 P. Wittenburg, K. Wolstencroft, J. Zhao, and B. Mons. The fair guiding principles for scientific data management and stewardship.
568 *Sci Data*, 3:160018, Mar 2016. doi: 10.1038/sdata.2016.18.